

**NEUTRONICS ANALYSIS FOR AN  
ACCELERATOR-BASED NUCLEAR WASTE TRANSMUTE**

William C. Sailor and Carl A. Beard  
Los Alamos National Laboratory  
Los Alamos, NM 87545

**ABSTRACT**

The neutronic analysis for a target/blanket design that is capable of supporting the high level waste stream from 2.5 LWR'S is described. The target consists of a set of solid tungsten and lead plates, cooled by heavy water and surrounded by a lead annulus. The annular blanket, which surrounds the target, consists of a set of AcO<sub>2</sub> slurry bearing tubes, each 3 meters long, surrounded by heavy water moderator. Heat removal from the slurry tubes is by passing the rapidly moving slurry through an external heat exchanger. There are separate regions for long-lived fission product burning. Using the Monte Carlo codes LAHET and MCNP we have optimized the design for a minimum beam current of 62.5 mA of 1.6 GeV protons.

**INTRODUCTION**

The central objective of Accelerator Transmutation of Waste (ATW) systems is to reduce the risk to the public from long-term geological storage of commercial light-water reactor (LWR) nuclear waste. The two main risks that are addressed by ATW are the migration of long-lived species in groundwater and the hazard from accidental intrusion. The risk in the first case can be taken to be dominated by the long-lived fission products <sup>99</sup>Tc and <sup>129</sup>I. These species have the undesirable properties of long half-lives, energetic radioactive decay, volatility in water, and non-retention in common soils by ion-exchange processes. In the second risk category, accidental intrusion into the repository, the hazard is dominated by species that are a contact hazard, i. e., the actinides. The most notable of these species are <sup>241</sup>Am and <sup>243</sup>Am, <sup>237</sup>Np, <sup>239</sup>Pu and <sup>240</sup>Pu. The Cm species are also of concern because they decay to Pu species. The actinides can also be considered as potential nuclear weapons material, and thus a lure for intentional intrusion into the repository. The very toxic species <sup>90</sup>Sr and <sup>137</sup>Cs will dominate the risk to the public on time scales of centuries, and this is not changed by ATW. The very Long-lived species <sup>238</sup>U and its decay daughters such as <sup>226</sup>Ra will dominate the repository intrusion hazard at times greater than 10<sup>5</sup> years, when the radioactivity has become very low. <sup>1</sup>

There may be some question as to the necessity of using such elaborate technology to reduce small risks still further, and whether the partitioning of the species will actually increase short-term risk to the public. However, the ATW system here produces an equivalent amount of electricity as a conventional nuclear power station, while having several safety advantages versus the LWR or LMFBR. In addition, the waste

stream from ATW contains no materials that can be used for nuclear weapons.

The feed to the ATW system (Figure 1) is thus the separated actinides Np, Pu, Am and Cm plus the long lived fission products (LLFP's) <sup>99</sup>Tc and <sup>129</sup>I. Chemical separation capacity is assumed to allow the LWR spent fuel to be partitioned into various streams before ATW is feasible. No isotopic separation is used, so that the stable species <sup>127</sup>I is transmuted along with the <sup>129</sup>I. The ATW target/blanket converts the LLFP's to stable species by neutron capture and the actinides to fission products by capture and fission. There is a small chemical facility to remove any LLFP's created by fission for recycle, and to continuously recycle the actinides.

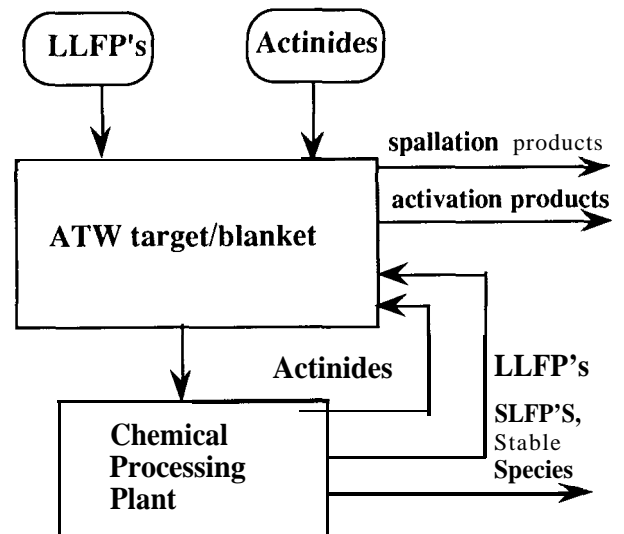


Figure 1. General concept of ATW system. The feed consists of long-lived fission products (LLFP's) and actinides. The output consists of stable species, short lived fission products (SLFP's), and some spallation and activation products.

Waste streams from ATW include the fission products from the transmutation of the actinides, spallation products from the target, and activation products from the structure of the ATW system. The fission product stream can be approximated as that for LWR discharge,<sup>2</sup> except that there will be no <sup>99</sup>Tc or <sup>127,129</sup>I present. The long-lived

spallation products  $^{182}\text{Hf}$ ,  $^{194}\text{Hg}$ ,  $^{202}\text{Pb}$ , and  $^{205}\text{Pb}$  are produced in the target at a rate of 0.020, 0.24, 1.83 and 4.2 moles/year, respectively. It is assumed that these species will be continuously recycled into re-manufactured targets and are continuously being transmuted at the rate at which they are produced. The activation products from the system are addressed in another paper in this conference.<sup>3</sup>

In exchange for producing these waste streams, the ATW target/blanket eliminates 3407, 613 and 136 moles per year of actinides,  $^{99}\text{Tc}$ , and  $^{127,129}\text{I}$ , respectively, from LWR waste. The net electrical production (after allowing for 200 MW<sub>e</sub> for operating the accelerator) is 400 MW<sub>e</sub>.

The target consists of a set of heavy water cooled tungsten and lead plates, surrounded by a lead annulus. The blanket is a heavy water moderated heterogeneous design, using a flowing slurry of actinide oxide ( $\text{AcO}_2$ ) in zirconium alloy tubes. Fission heat is carried away by convection and the slurry is cooled in an external heat exchanger. There are separate regions in the blanket for LLFP transmutation. We envision four of these target/blanket assemblies per 250 mA accelerator (1.6 GeV beam), and thus we hold the beam current per target/blanket at 62.5 mA. Overall system economics is discussed in another paper in this conference.<sup>4</sup> Much of the aqueous slurry and solution reactor experience of the last 40 years will be applicable to our concept.<sup>5,6</sup>

In this paper we describe the conceptual design of a target/blanket assembly that performs as part of a system as

described above. Calculations are for steady-state and time-dependent neutron economy, coupled with actinide composition calculations. Most of our results rely on the code MCNP.<sup>7</sup>

### ACTINIDE REACTIONS

Figure 2 shows the 25 actinide species that we normally take to constitute the fuel in a waste burner. Each of the four elements constitutes a chain of species that must be taken to terminate at some endpoint. We allow each species to be labeled with a number, where 1 implies  $^{237}\text{Np}$ , and 25 implies  $^{249}\text{Cm}$ . The governing equation for the number of moles of species  $k$  implied by Figure 1 is:

$$\frac{dN_k}{dt} = F_k - \lambda_k N_k - \phi \sigma_k N_k + \sum_{i=1}^{25} \sigma_{i \rightarrow k} \phi N_i + \sum_{i=1}^{25} \lambda_{i \rightarrow k} N_i$$

where  $N_k$  is the number of moles,  $F_k$  is the feed rate,  $\lambda_k$  the decay constant for species  $k$  to all channels,  $\phi$  the flux,  $\sigma_k$  the capture plus fission cross section. The summations are feed terms from decay and capture on other actinides. Thus  $\sigma_{i \rightarrow k}$  is the cross section for the capture on species  $i$  leading to species  $k$ , and  $\lambda_{i \rightarrow k}$  is the decay constant for species  $i$  leading to species  $k$ . These constants contain the branching ratios, e. g., if the  $^{241}\text{Am}$  capture cross section is 10 barn, the cross section leading to  $^{242}\text{Am}$  is 8 barn and the cross section leading to  $^{243}\text{Am}$  is 2 barn.

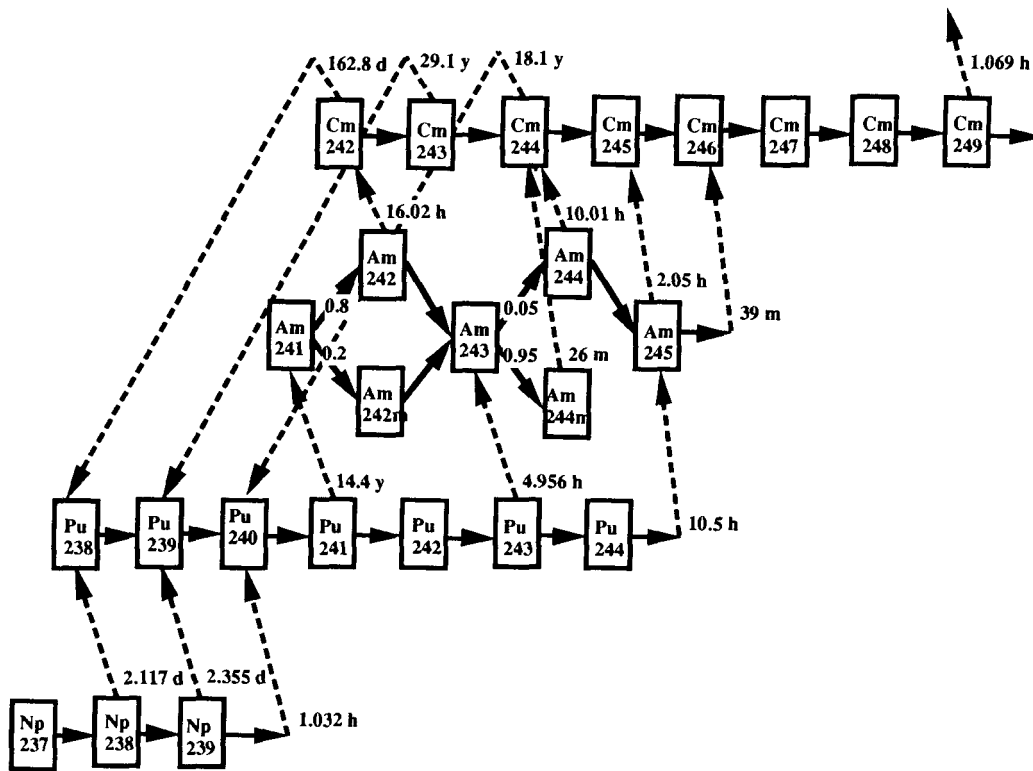


Figure 2. The calculations consider these reactions and decays in the actinides.

To model the entire 25 species, there are 25 such equations coupled by the summation terms. The coupling is sparse: there are at most 2 terms in each summation that are non-zero, according to Figure 2. Now the following model assumptions are made:

$$(2) \phi = \phi^{SS} \quad \text{and} \quad N_k = S_k$$

i. e., the flux in the system is fixed at a steady state value. The system responds by equilibrating at steady state concentrations  $S_k$ . We substitute the assumptions into the system of equations implied by (1) and we obtain:

$$(3) 0 = F_k - \lambda_k S_k - \phi \sigma_k S_k + \sum_{i=1}^{25} \sigma_{i \rightarrow k} \phi S_i + \sum_{i=1}^{25} \lambda_{i \rightarrow k} S_i$$

The solution to (3) gives the steady state concentrations. These concentrations are, in general, much different than the initial feed. In Figure 3a we show the feed and equilibrium atom fractions for the commercial waste burner. The equilibrium composition depends, of course, on the 1-group cross sections and flux level in the blanket, as well as the chemical processing assumptions. The results in this figure correspond to the final design presented here. Although the feed is 51%  $^{239}\text{Pu}$ , the equilibrium fraction is only about 3%. At equilibrium, the species  $^{242}\text{Pu}$ ,  $^{243}\text{Am}$ , and  $^{244}\text{Cm}$  make up the majority of the composition. It is no coincidence that these species tend to have rather small cross sections.

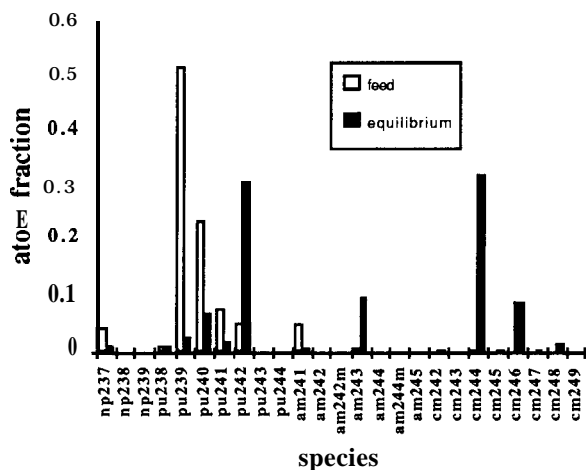


Figure 3a. Atom fractions of the actinides in the feed and at equilibrium. The distributions are quite different.

Figure 3b shows the rates of decays, captures and fissions that each species undergo at equilibrium. The fissions are taking place in  $^{239}\text{Pu}$  and  $^{241}\text{Pu}$  predominantly, with about 9% occurring in  $^{245}\text{Cm}$ . Some fast fission occurs in the even-numbered Pu and Cm isotopes, and in the highly fissile  $^{242m}\text{Am}$ . The Pu species also undergo most of the capture reactions, except for  $^{243}\text{Am}$  and  $^{244}\text{Cm}$ .

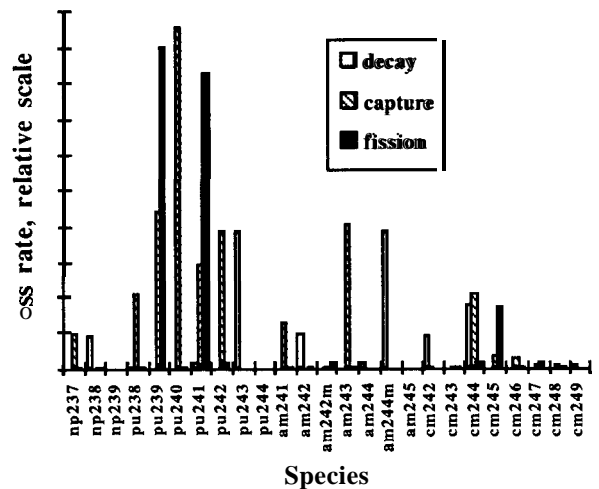


Figure 3b. Loss rates of the species to decay, capture and fission at equilibrium. The main species undergoing fission are  $^{239}\text{Pu}$ ,  $^{241}\text{Pu}$ , and  $^{245}\text{Cm}$ .

One of the basic hypotheses of ATW is the desire to maintain a high thermal flux.<sup>8</sup> The purpose is to fission short lived fissile species before they decay. A case in point is  $^{241}\text{Pu}$ , which has, in our spectrum, a fission cross section of 240 b. The flux level where the fission rate is equal to the decay rate is  $6.3 \times 10^{12} \text{ n/cm}^2/\text{s}$ . Calculations (Figure 4) of the equilibrium fuel capture-to-fission ratio,  $\alpha$ , as a function of flux level show that for a fixed spectrum the ratio vanes only slowly unless the flux approaches this value.

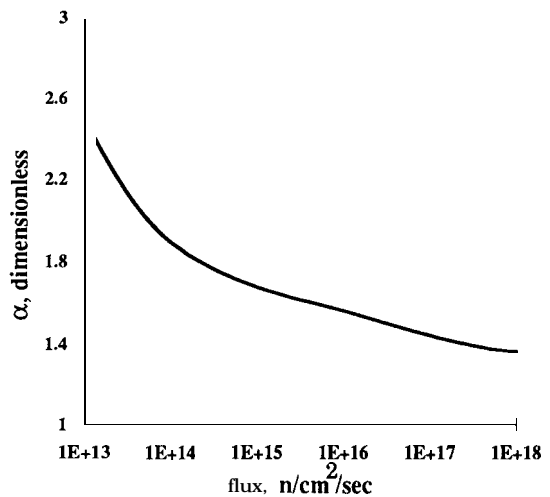


Figure 4. Lumped actinide  $\alpha$  value variation with flux level in ATW system, using the 1-group cross sections from the final design. Our designs have been near  $10^{15} \text{ n/cm}^2/\text{sec}$ , where the curve is fairly flat.

Most of our designs use flux levels at or near  $1 \times 10^{15}$  n/cm<sup>2</sup>/sec, where the curve is fairly flat at  $a = 1.60 \pm 0.04$ . The continuously downward trend in  $a$  with increasing flux is due to the increasing fission rate of minor species such as <sup>238</sup>Np.

In most of our calculations we assume steady-state. However, the approach to steady-state has also been calculated by coupling MCNP with ORIGEN2.<sup>9</sup> In the calculations we use a constant power density in the actinide fuel of 0.8 kW/g, which is the same power density that we have calculated at equilibrium. The initial feed is sent into the blanket and the cross sections are calculated. These cross sections are written to a file that is read in by ORIGEN2. A forward time step is performed by ORIGEN2, solving the complete set of coupled ODES as defined in equation (1). A new concentration is obtained. These time steps are typically a few days. After enough of these steps are performed, a full year of operation has been simulated. The ORIGEN2 calculations are temporarily stopped, a new MCNP input file is written, and the cross sections are again calculated. By repeating this process, we can track the entire approach to equilibrium in a self-consistent fashion.

The time dependence of the isotopic fractions is illustrated in Figure 5. The feed is 51% <sup>239</sup>Pu, decreasing to about 3.17% at 40 years. Two other species, <sup>242</sup>Pu and <sup>246</sup>Cm are also shown for comparison. There is little of these species present in the feed, but they grow to significant fractions at 40 years time. Equilibrium  $a$  value of about 1.62 is reached in about 18 years. The lumped average fission cross section for the actinides is about twice as high at beginning of life compared to equilibrium. Therefore, for a constant power density, the flux will vary by a factor of two over the life of the plant.

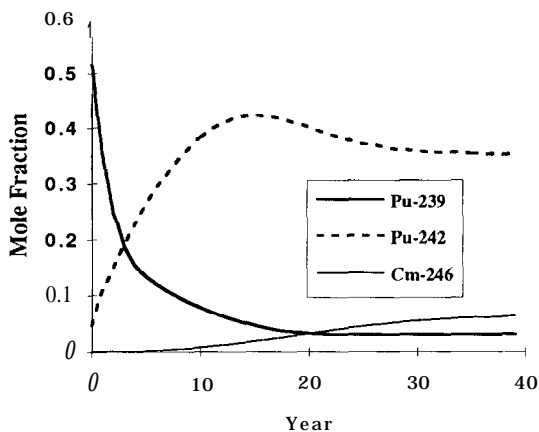


Figure 5. Time dependence of some of the actinide species in ATW system. At startup, the actinides are 51% <sup>239</sup>Pu, but this reduces eventually to about 3%. There is essentially no <sup>246</sup>Cm at startup, but this builds up to about 7% at 40 years time.

## EFFECTS OF CONCENTRATION AND PITCH

Our basic design (Figure 6) employs a lattice of double-wall Zr (97.5%)-Nb(2.5%) tubes which contain a heavy water slurry of 5-50 μm actinide oxide (AcO<sub>2</sub>) particles. Outside the tubes is a heavy water moderator, thermally isolated from the slurry by the gap between the tubes. From fission there is a large volumetric heat generation. The heat is earned away by convection, and the slurry is cooled in an external heat exchanger. As mentioned in the introduction, there is a chemical processing plant to remove the fission products, and we assume a 50% residence time for Am and Cm in this system, and a 25% residence time for Pu and Np. Another paper at this conference explains in detail the processing assumptions.<sup>10</sup>

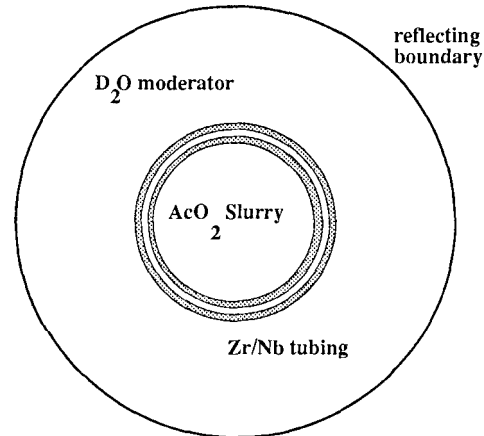


Figure 6. Unit cell used in lattice calculations. There are two walls of Zr (97.5%) - Nb (2.570) alloy, each 3.25 cm thick. The inner radius is 3.87 cm. The cell radius is 10.53 cm, corresponding to a pitch of 20 cm in a hexagonal lattice.

This section summarizes the results of equilibrium heterogeneous unit cell calculations. All results here use MCNP, coupled with a code that solves the system implied by equation (3). The part of the program which calculates equilibrium actinide concentrations was written so that the power density was held constant at 700 MW/m<sup>3</sup> in the slurry tubes. This represents a thermal/hydraulic limit, i. e., the fluid velocity in this convective system (which is proportional to the volumetric power density) is about 10- 12 m/s.

The tubing we use has its thickness chosen for a 13.1 MPa operating pressure. The outer radius of the unit cell, which is reflecting, corresponds to a pitch between tubes of 20 cm in a hexagonal lattice. Other calculations, not shown here in detail, varied the radius of the unit cell and/or the radii of the tubes. Here we present only the results of varying the concentration for a given geometry. The moderator is at room temperature and density, while the D2O carrier for the slurry was at 300 C and a density of 0.7 g/cm<sup>3</sup>.

The individual fission and capture cross sections are generally a decreasing function of concentration and increasing function of inter-tube pitch. For instance, for a concentration variation between 100 g/l and 600 g/l the <sup>239</sup>Pu fission cross section drops from 550 barn to 275 barn (the results are at a fixed power density of 700 MW/m<sup>3</sup>). The

lowered cross sections at higher loadings are the result of thermal flux depression within the tube. Increasing the pitch of the cell softens the spectrum, with the result that the cross section is four times as great with a 30 cm pitch as at a 15 cm pitch. If all cross sections of importance varied with  $I/v$ , the capture-to-fission ratios for each species would be independent of pitch or concentration. It is found that because of non- $I/v$  behavior, there are some departures from this, e. g., the capture-to-fission ratio for  $^{239}\text{Pu}$  shows a slight increase with concentration, while for  $^{241}\text{Pu}$  the trend is the opposite.

We have included the effect of capture of neutrons on the fission products that are present in the slurry. The fraction of neutrons that are lost to these captures varies with the flux and the mean residence time before removal for processing. We performed model calculations using the code **ORIGEN2**, and parameterized the results to include in our unit cell and full blanket MCNP calculations. For the flux level here and a 26 day residence time in the blanket, the ratio of these fission product captures to fission events is about 0.12.

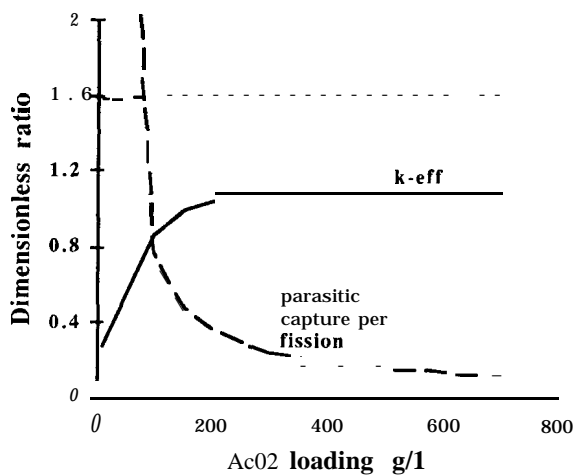


Figure 7. Dimensionless ratio variation with concentration in unit cell calculations. The power density in the slurry is  $700 \text{ MW/m}^3$ .

Some parameters of importance are plotted versus loading in Figure 7. The lumped actinide  $\lambda$  value is flat. But the important ratio of parasitic capture (in the tubing and the moderator) per fission (given the symbol  $\phi_p$ ) is a strong function of concentration, decreasing to tolerable levels only at  $300 \text{ g/l}$  or more. The resulting  $k$ -eff for the reflecting (and therefore the infinite lattice) case is an increasing function of concentration, reaching a value of 1.07 at  $700 \text{ g/l}$  loading. Based on these and other calculations, we chose a slurry loading of  $500 \text{ g/l}$  and a pitch of  $20 \text{ cm}$  between tubes in a hexagonal lattice. The main reason for choosing such a high loading is to reduce the effect of parasitic capture, as is illustrated in the previous figure. This high loading also tends to reduce the parasitic capture in the target per fission. The results of full-blanket calculations are in a later section.

## SPALLATION TARGET

The ATW accelerator target is a modification of the split-composite W/Pb spallation target design<sup>1</sup> which is composed of solid tungsten and lead, cooled by heavy water. The target is cylindrical in configuration, with two radial regions. The inner radial region ( $0 \text{ cm} < r < 16 \text{ cm}$ ) contains a series of tungsten plates spaced in order to optimize neutron leakage, reduce parasitic absorption in the tungsten, and axially distribute the neutron source to reduce the axial flux peaking in the blanket. The outer radial region ( $16 \text{ cm} < r < 27 \text{ cm}$ ) is a lead annulus which generates neutrons from protons scattered outside of the tungsten region. At the back of the target is a lead beam stop extending through both radial regions which is used to range out the beam. The target is shown in Figure 8.

The LAHET Code System<sup>12</sup> (LCS) was used to characterize the neutron source generated in the split-composite W/Pb target, and also to perform fully coupled LAHET/MCNP calculations on the entire system. LAHET uses the Intranuclear Cascade/Evaporation model to predict high-energy interactions, and writes a source tape of the resulting particles (both neutrons and photons) for subsequent transport in the Monte Carlo transport code MCNP<sup>3</sup>. For  $1600 \text{ MeV}$  protons, the LCS predicts a total neutron source of  $40.32$  neutrons/proton. Table 1 shows the neutron leakage from the bare target, and the average energy of the escaping neutrons, although neutrons which enter the heavy water moderator are quickly thermalized. Figure 9 shows the axial distribution of the neutron leakage across the outer surface of the lead annulus for the bare split-composite target. The neutron source emitted from the active portion of the target (beyond the first tungsten plate) has a fairly even axial distribution, especially when compared with homogeneous solid targets or liquid heavy metal targets (e.g. liquid lead or lead-bismuth) which produce highly localized sources of neutrons and typically have problems with neutron leakage off the front target face.<sup>13</sup>

Table 1: Neutron Leakage from Bare Split-Composite W/Pb Target

Surface	Leakage (neutrons per proton)	Average Neutron Energy (MeV)
Front	0.143	
Back	1.919	17.78
Radial	34.22	6.041

The main disadvantage of this target is the presence of the lead which produces a mixed waste, complicating target disposal. While activation in the lead is low, the spallation process generates the long-lived isotopes  $^{202}\text{Pb}$ ,  $^{205}\text{Pb}$ , and  $^{194}\text{Hg}$ , whose half-lives and spallation yields are given in Table 2. Since  $^{205}\text{Pb}$  is the long-lived nuclide produced in the greatest amount (not only due to its high spallation yield as shown in Table 2, but also due to its production from capture in stable  $^{204}\text{Pb}$  which is present in naturally occurring lead), its equilibrium amount was estimated using characteristic system parameters. A total of  $22 \text{ kg}$  of  $^{205}\text{Pb}$  is produced in the system, with it reaching  $95\%$  of its equilibrium in  $21.5$  years.

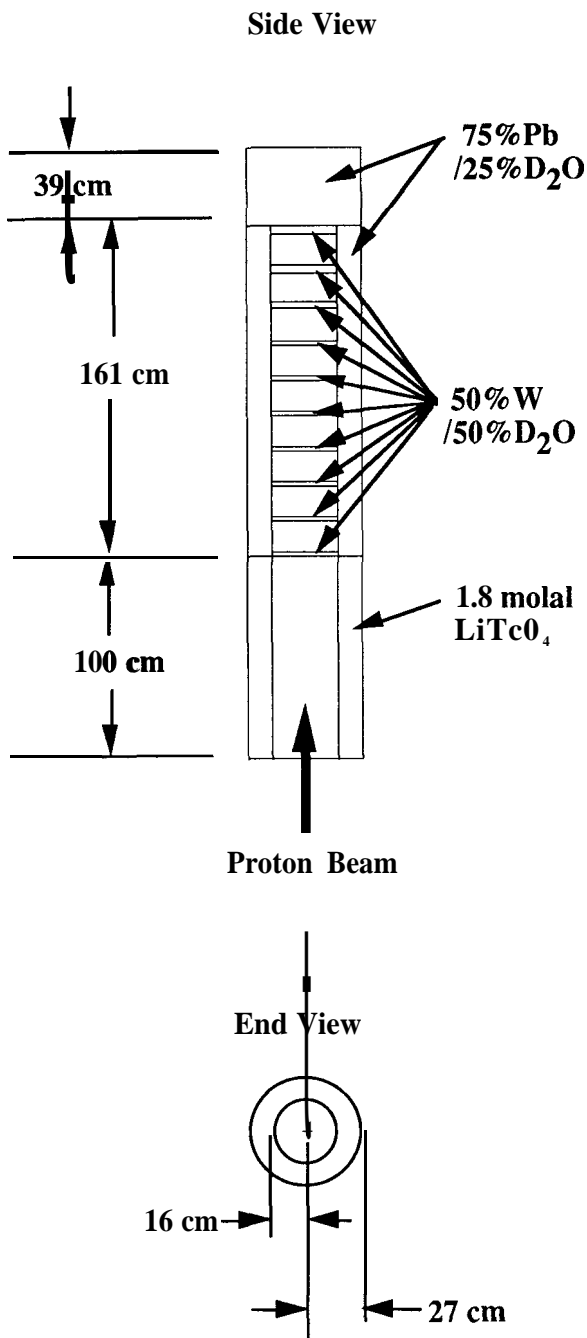


Figure 8. The split-composite W/Pb spallation target for the ATW blanket.

#### WHOLE-BLANKET RESULTS

The results of the unit cell calculations were used to estimate the neutronic performance in a whole blanket. The code MCNP was used in a source mode calculation, configured to read in the source resulting from the LAHET target calculations. Borrowing from the above lattice calculations, a 500 g/l AcO<sub>2</sub> loading was chosen, with tubes as described above. The pitch was chosen as 20 cm.

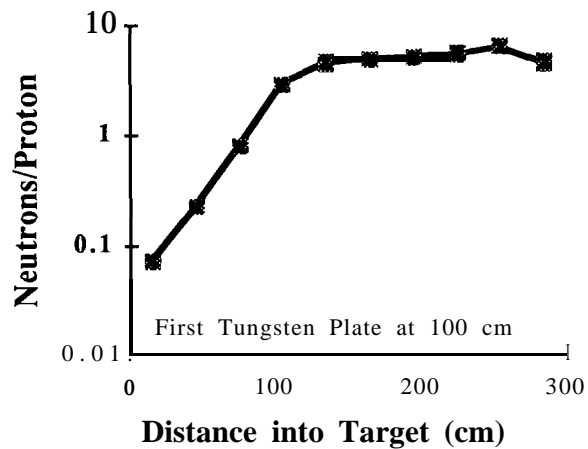


Figure 9. Axial distribution of radial neutron leakage

Table 2: Spallation Yields of Long-Lived Isotopes Produced in the Target Lead

Isotope	Half-Life (years)	Spallation Yield (atoms per proton)
Hg <sup>194</sup>	520	0.0209
Pb <sup>202</sup>	53000	0.1567
Pb <sup>205</sup>	1.51e+07	0.3628

Separate LLFP transmutation regions were included in the blanket. One is located between the lead annulus and the slurry lattice, and the other is in the outer regions. The inner region prevents the diffusion of thermal neutrons from the lattice into the target region where they would otherwise be lost to parasitic capture. The outer LLFP region captures neutrons that would otherwise be lost to leakage.

The various dimensions of the blanket were adjusted to give a fission product/actinide burn rate of 0.28, while attempting to minimize parasitic capture in the target and moderator. This ratio is sufficient to burn the <sup>99</sup>Tc and <sup>127, 129</sup>I from LWR discharge, and from the fission yields of the actinides.

Design dimensions are given in Table 3. A description of the blanket is given in Figure 10. Because of the somewhat tight pitch, we were able to fit 186 tubes into the blanket. The flux is 1.7x10<sup>15</sup>, producing a power density of 700 MW/m<sup>3</sup> of slurry.

Table 3. The final ATW target/blanket design summary based on coupled whole-blanket MCNP calculations and equilibrium actinide concentrations.

specified power density, $MW/m^3$	700.00
average flux in the actinide regions, $n/cm^2/sec$	$1.70 \times 10^{15}$
temperature of slurry (C)	300.0000
temperature of moderator (C)	100.0000
height of blanket (cm)	300.0000
outer radius of target region (cm)	15.5000
inner radius of cylindrical lead region (cm)	16.0000
inner radius of inner technicium region (cm)	27.0000
outer radius of inner technicium region (cm)	33.0000
outer radius of multiplying region (cm)	190.0000
outer technicium region thickness (cm)	7.0000
heavy water outer reflector thickness (cm)	30.0000
radius where actinide tubes begin (cm)	40.0000
pitch (cm)	20.0000
actinide tube inner radius (cm)	3.8700
actinide concentration, $g/l$ ${}^7LiTcO_4$	500.0000
concentration, molal	1.8000
Fraction of time in HX	.5000
Fraction of time in processing (Np)	.2500
Fraction of time in processing (Pu)	.2500
Fraction of time in processing (Am)	.5000
Fraction of time in processing (Cm)	.5000
Number of days for FP processing	26.0000
number of actinide tubes in blanket	186
Blanket Actinide Inventory, kg	1300
kgs. Tc	835
total multiplication	13.6
parasitic capture-to-fission ratio	0.18
leakage-to-fission ratio	.05
LLFP capture-to-fission ratio	.280
Ac capture-to-fission ratio	1.64
Actinide bum rate, LWR equiv.	2.5
Required beam current, mA	62.5

The total parasitic-capture-to-fission ratio is found to be 0.18. Of this 0.18, it is found that 0.08 is from the slurry tubing, 0.03 from the moderator, 0.01 from the lead and 0.06 from tungsten. Roughly half of the LLFP burning comes from the inner decoupler region. The value for  $\alpha$  was found to be 1.64, slightly higher than indicated by the unit cell calculations. The blanket holds 1300 kg of Ac<sub>2</sub>, and burns this at a rate of 70% per year. There are a total of 500 neutrons from all sources, including fission, per 1.6 GeV proton on the target.

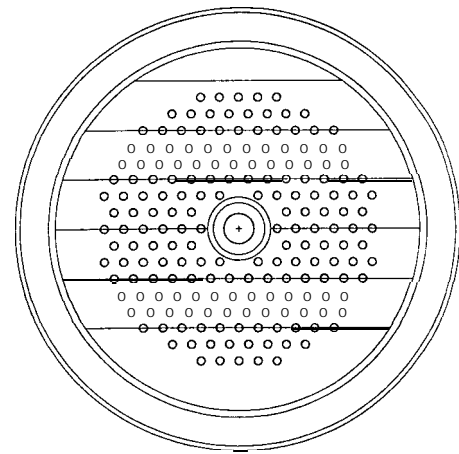
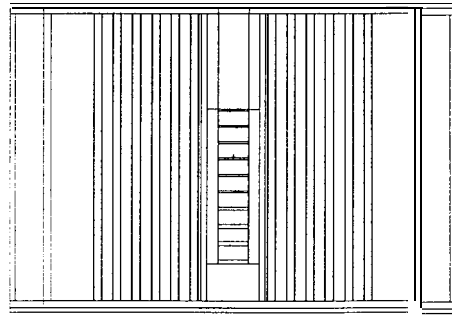


Figure 10. Top and side views of the ATW blanket. The target is in the center, followed by a lead annulus and inner LLFP region, followed by the multiplying lattice, the outer LLFP region, and then the reflector and outer stainless steel wall.

### SLURRY PROPERTIES AND EROSION

There have been objections to the high slurry loadings on the basis of erosion. The power density here also gives a high slurry velocity. Our neutronics calculations have always taken this into consideration, and we have attempted to keep the flow velocities in the 10 m/s range.

The velocity required for the slurry in the tubes can be calculated from an enthalpy balance on the tubes, assuming that the entrance and exit temperatures for the slurry are fixed at 275 C and 325 C, respectively. The resulting velocity and concentrations are essentially typical of those where experimental erosion data are available.

The erosion of materials by slurries has been measured for concentrations up to 1500 g/liter, at temperatures typically between 500 K and 600 K, and flow velocities up to 30 m/s. In general, the erosion rate is a strong function of particle size and shape, and is affected to a lesser degree by oxygen overpressure, solution acidity, slurry concentration, slurry temperature, and flow velocity. Optimum particle size is between 1 and 5 microns, with smooth particles causing less erosion. Using particles fabricated with these characteristics,

the erosion rate of 450 g/liter  $\text{ThO}_2$  at 553 K and flowing at 6 m/s was measured to be less than 0.5 mils/yr for zirconium, and approximately 3 mils/yr for stainless steel. 14 For 1500 g/liter at 553 K and 12.2 m/s, the erosion rate on zirconium was 1 mil/yr.<sup>15</sup> Erosion rates for the zirconium slurry tubes in the aqueous ATW system are therefore expected to be less than 1 mil/year. The tubes will have to be replaced every -10 years.

## CONCLUSIONS

In a conceptual design it is possible to burn the actinides,  $^{129}\text{I}$  and  $^{99}\text{Tc}$  from 2.5 LWR's in an ATW target/blanket assembly using 62.5 mA of current and aqueous technology. The heat from the blanket is sufficient to generate 600 MW of electrical energy at the expected 30% thermal-to-electrical conversion efficiency. Since about 200 MW is expected to be needed to run the accelerator (at 50% wall plug efficiency), this leaves 400 MW of electrical energy to be sold to the grid.

The waste streams are very radioactive, but the species are typically short lived. The only long-lived species in the waste stream do not pose a migration or intrusion hazard for a geological repository.

The tools we have developed to analyze this target/blanket design will enable us to move into an ever-wider area of conceptual designs. For instance, the burning of commercial waste can be combined with a fertile feed, breeding fissile material. Other moderators may give different, more favorable spectral characteristics. The improved neutron economy of these changes will translate into a lower cost of producing electricity from the burning of nuclear waste.

## REFERENCES

1. L. C. HEBEL, Chrmn., "Report to the American Physical Society by the study group on nuclear fuel cycles and waste management", Rev. Mod. Phys. Vol. 50, No. 1, Part II, 1978.
2. M. BENEDICT, T. H. PIGFORD, AND H. W. LEVI, Nuclear Chemical Engineering, Second Edition, McGraw-Hill, 1981, pages 352-406.
3. J. BEZDECNY, "Radionuclide Formation in Four Structural Regions of the Base Case Aqueous ATW Reactor", this conference.
4. R. KRAKOWSKI, "AT W Economics", this conference.
5. J. A. LANE, H. G. McPHERSON, AND F. MASLAN, Fluid Fuel Reactors, Addison-Wesley, Reading, MA, 1958.
6. "Final report on the aqueous homogeneous suspension reactor project", Kema Scientific and Technical Reports 5 (1): 1 - 48 (1987). Available from the National Technical Information Center, Springfield, VA, 22161.
7. J. F. BREISMEISTER, Ed, "MCNP-A General Monte Carlo Code For Neutron And Photon Transport", Los Alamos National Laboratory, Los Alamos, New Mexico, LA-7396-M, Rev. 2, September, 1986.
8. C. D. BOWMAN, et. al., Nucl. Inst. Meth. A320 (1992) pp. 336.
9. A. G. CROFF, "A user's manual for the ORIGEN2 computer code", July, 1980. Available from the Radiation Shielding and Information Center, Oak Ridge National Laboratory, Post Office Box X, Oak Ridge, TN 37831.
10. J. W. DAVIDSON AND M. E. BATTAT, "Neutronics-processing interface analyses for the Accelerator Transmutation of Waste (ATW) Aqueous-Based Blanket System", this conference.
11. G. RUSSEL, Los Alamos National Laboratory, personal communication.
12. R. E. PRAEL and H. LICHTENSTEIN, "User Guide to LCS: The LAHET Code System," LA-UR-89-3014, Los Alamos National Laboratory (September 1989).
13. C. A. BEARD, PhD Thesis, Texas A&M University, Dept. of Nuclear Engineering, 1992.
14. W. E. BERRY, Corrosion in Nuclear Applications, John Wiley and Sons, Inc., New York (1971).
15. "Aqueous Homogeneous Reactor Fuel Technology," Proceedings of the Second International Conference on the Peaceful Uses of Atomic Energy, Vol. 7. Reactor Technology, pp. 3-20.